Bulgarian Journal of Physics vol. **46** (2019) 347–353

Rod-Shaped Nuclei in Covariant Density Functional Theory

Z.X. Ren, **P.W. Zhao**

[1]State Key Laboratory of Nuclear Physics and Technology, School of Physics, Peking University, Beijing 100871, China

Received *20 November 2019*

Abstract. The realization of anomalously rod-shaped nuclei has been a long-standing objective of nuclear structure physics. In this contribution, the linear-chain structure with a rod shape in carbon isotopes is discussed within the framework of cranking covariant density functional theory. In particular, the effects of spin and isospin, and their interplay are discussed in details.

KEY WORDS: Rod-shaped nuclei, Linear-chain structure, Alpha-cluster structure, Carbon isotopes, Cranking covariant density functional theory

1 Introduction

Strong nuclear deformations provide us an excellent framework to investigate the fundamental properties of quantum many-body systems. The strong deformation in heavy nuclei with width-to-length ratios of 1:2 or 1:3 has been identified by the observed superdeformed [1, 2] and hyperdeformed bands [3–5]. In light nuclei, more exotic linear-chain structure with a rod shape might exist in nuclei due to the appearance of the α cluster structure.

The linear-chain structure of three α clusters was suggested in ^{12}C about 60 years ago [6] for the structure of the Hoyle state (the second 0^+ state with excitation energy $E_x = 7.65$ MeV). Although later investigation indicates that Hoyle state was a gas-like state with strong mixing of the linear chain and other configurations [7] and recently reinterpreted as an α-condensate-like state [8, 9], the linear-chain cluster state still attracts great attentions from nuclear physicists. Various theoretical and experimental studies of linear-chain states have been carried out in not only ^{12}C [10–14], but also other $N = Z$ nuclei, such as ^{16}O [15–17], ^{24}Mg [18–21], etc.

Due to the antisymmetrization effects and the weak-coupling nature, the linear-chain configuration with a rod shape is difficult to be stabilized against bending motion. To stabilize this exotic configuration, some extra mechanisms have been introduced. One possible mechanisms is increasing isospin by adding valence neutrons. In particular, if the so-called σ orbital is occupied by neutrons, an elongated shape for the core would be favored to lower the energy of the valence neutrons [22]. Another possible one is increasing spin by rotating the nucleus rapidly, because the linear-chain configuration with a large moment of inertia could be energetically favoured with a high spin [23].

For the theoretical analyses of the linear-chain structure, most of them are performed by using the conventional cluster model [24]. Recently, the cranking covariant density functional theory (CDFT) has also been used to investigate the linear-chain structures in carbon isotopes [10, 11]. The effects of extreme spin and isospin were simultaneously discussed for the first time in a self-consistent and microscopic way. By adding valence neutrons and rotating the system, the σ orbitals of the valence neutrons were lowered by the rotation [10]. With adopting the technology of solving Dirac equation in three-dimensional (3D) lattice space [25], the linear-chain structure with a high spin was found to be stabilized against bending motion [11].

In this contribution, the cranking CDFT investigations for the linear-chain structures in carbon isotopes are presented and the effects of valence neutrons and rotation are discussed in details.

2 Results and Discussions

In Figure 1, the single-neutron levels in the rotating frame together with their occupation are shown for the nucleus ^{15}C with a linear-chain configuration, where the equation of motion is solved in a 3D Cartesian harmonic oscillator basis; see Ref. [10] for details. The Nilsson quantum numbers $\Omega[Nn_z\Lambda]$ in Figure 1 give the maximal component of each level, and solid and dashed lines denote the positive and negative parities, respectively. It should note that the densities of the levels with small Λ values are close to the symmetry axis, while those with large Λ values are away from the symmetry axis.

As shown in Figure 1, the valence neutrons occupy the levels with $\Lambda = 1$ at the rotational frequency $\hbar\omega = 0$, which contributes an oblate distribution. With the increase of $\hbar\omega$, the $1/2[330]$ orbital drops rapidly and starts to be occupied after the level crossing near $\hbar\omega = 1.75$ MeV. Such an orbital is the so-called σ orbital, and would contribute a prolate distribution to the neutron density. As discussed in Ref. [10], this indicates the spin and isospin effects, which enhance the stability of the rod-shaped configuration.

For the stability of linear-chain structure against bending motion, the 3D lattice solution of the cranking CDFT is adopted. Starting from a twisted three α initial [see the initial state in Figure 2], the self-consistent cranking CDFT calculations at various rotational frequencies $\hbar\omega$ are performed for the nucleus ^{12}C. The numerical details for the calculations can be found in Ref. [11]. Figure 2 shows the

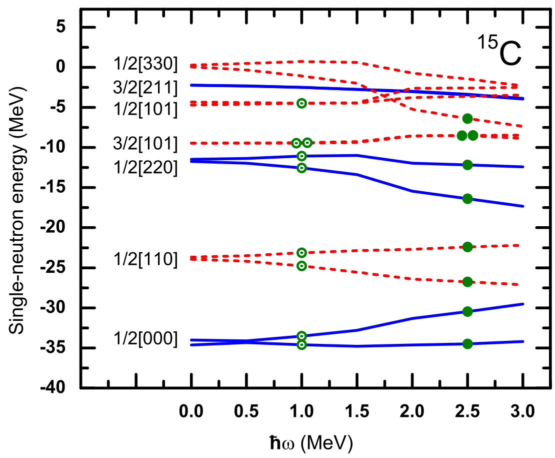

Figure 1. Neutron single-particle energies (in rotating frame) as functions of the rotational frequency for ^{15}C. The open and solid circles denote, respectively, the occupied orbitals before and after the level crossing near $\hbar\omega = 1.75$ MeV. Taken from Ref. [10].

evolution of the coefficient of the rotational energy $\hbar^2/2\Im_{\rm rigid}$, where the moment of inertia is evaluated by the rigid body formula $\Im_{\rm rigid} = m_N\langle x^2 + z^2\rangle$.

As discussed in Ref. [11], the final states are classified into three groups according to the final values of $\hbar^2/2\Im_{\rm rigid}$: (a) ground state for $\hbar\omega = 0.5$, 1.0 and 1.5 MeV, (b) linear-chain states for $\hbar\omega = 2.0$ to 3.5 MeV, and (c) fission for $\hbar\omega = 4.0$ MeV. At rotational frequencies $\hbar\omega = 0.5$, 1.0 and 1.5 MeV, the linear-

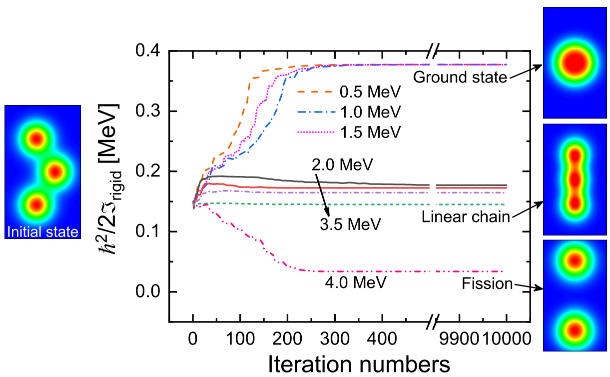

Figure 2. Coefficient of the rotational energy, $\hbar^2/2\Im_{\rm rigid}$, calculated by cranking CDFT in 3D lattice space for the nucleus ^{12}C as a function of iteration numbers at rotational frequencies $\hbar\omega = 0.5$, 1.0, ..., 4.0 MeV. The insert density distributions correspond to the the initial state, ground state, linear-chain state, and fission. Taken from Ref. [11].

chain state is not stable against the bending motion, and finally it turns into the ground state. With the increasing rotational frequency (2.0 to 3.5 MeV), the strong centrifugal force stabilizes linear-chain states against the bending motion. In particular, because the 3D lattice cranking CDFT calculations do not have any symmetry restriction, the obtained linear chain solution corresponds to a minimum in the energy surface with respect to bending motion. This shows that rotation can stabilize the linear-chain structure. The fission occurs when the rotational frequency approaches $\sim$4.0 MeV.

In Figure 3, the angular momenta for the linear-chain states of ^{12}C are shown as a function of rotational frequency $\hbar\omega$. For a comparison, the results of the H.O. basis expansion method [10] are also presented, where the reflection symmetry is imposed. As seen in Figure. 3, except at $\hbar\omega = 3.5$ MeV, the angular momentum almost increases with $\hbar\omega$ linearly, which reveals that the moments of inertia $\Im$ are nearly constant below $\hbar\omega = 3.0$ MeV. Up to $\hbar\omega$=3.0 MeV, the results of 3D lattice and H.O. basis calculations are almost identical. For the deviation at $\hbar\omega$=3.5 MeV, it may be attributed to the smaller model space adopted in the H.O. basis calculations compared to the 3D lattice calculations. Ignoring results at $\hbar\omega = 3.5$ MeV, the moments of inertia $\Im$ can be obtained as 2.87 $(\text{MeV})^{-1}\hbar^2$ and 2.81 $(\text{MeV})^{-1}\hbar^2$ for 3D lattice and H.O. basis calculations, respectively. As mentioned in Ref. [11], this demonstrates that the results of 3D lattice and H.O. basis calculations are consistent with each other.

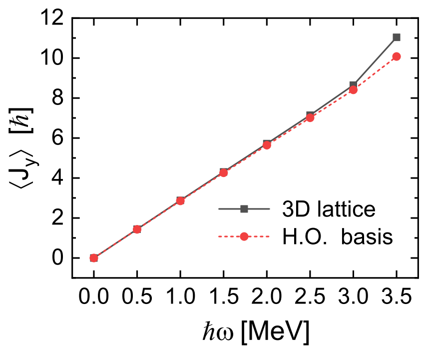

Figure 3. Angular momentum for the linear-chain states of ^{12}C as a function of rotational frequency $\hbar\omega$. The solid lines denote the results of 3D lattice calculations. The dashed lines show the results of harmonic oscillator (H.O.) basis expansion method with 12 major shells [10]. Taken from Ref. [11].

3 Conclusion

In summary, the exotic linear-chain structure with a rod shape in carbon isotopes is discussed within the framework of the cranking covariant density functional theory, where H.O. basis and 3D lattice calculations are adopted. With adding valence neutrons and rotating the system, the σ orbitals of the valence neutrons in ^{15}C are lowered by the rotation. Starting from a twisted three α initial configuration, the linear-chain structures in ^{12}C can be stabilized against bending motion when the rotational frequency is in the interval 2 MeV $< \hbar\omega <$ 3.5 MeV. In particular, the results of 3D lattice and H.O. basis calculations are consistent with each other.

Finally, it is worthwhile to mention that the microscopic dynamics of the linear-chain cluster states have also been discussed recently by the newly developed time-dependent covariant density functional theory in 3D lattice space [26].

Acknowledgements

We thank J. A. Maruhn, J. Meng, N. Itagaki, and S. Q. Zhang for helpful discussions and for the collaborations of the works discussed in this contribution. This work was partly supported by the National Key R&D Program of China (Contracts No. 2018YFA0404400 and No. 2017YFE0116700) and the National Natural Science Foundation of China (Grants No. 11621131001, No. 11875075, No. 11935003, and No. 11975031).

References

[1] B.M. Nyakó, J.R. Cresswell, P.D. Forsyth, D. Howe, P.J. Nolan, M.A. Riley, J.F. Sharpey-Schafer, J. Simpson, N.J. Ward, and P.J. Twin (1984) Observation of Superdeformation in ^{152}Dy. *Phys. Rev. Lett.* **52** 507
DOI: https://link.aps.org/doi/10.1103/PhysRevLett.52.507.

[2] P.J. Twin, B.M. Nyakó, A.H. Nelson, J. Simpson, M.A. Bentley, H.W. Cranmer-Gordon, P.D. Forsyth, D. Howe, A.R. Mokhtar, J.D. Morrison, J.F. SharpeySchafer, and G. Sletten (1986) Observation of a Discrete-Line Superdeformed Band up to $60\hbar$ in ^{152}Dy. *Phys. Rev. Lett.* **57** 811
DOI: https://link.aps.org/doi/10.1103/PhysRevLett.57.811.

[3] A. Galindo-Uribarri, H.R. Andrews, G.C. Ball, T.E. Drake, V.P. Janzen, J.A. Kuehner, S.M. Mullins, L. Persson, D. Prevost, D.C. Radford, J.C. Waddington, D. Ward, and R. Wyss (1993) First evidence for the hyperdeformed nuclear shape at high angular momentum. *Phys. Rev. Lett.* **71** 231
DOI: https://link.aps.org/doi/10.1103/PhysRevLett.71.231.

[4] D.R. LaFosse, D.G. Sarantites, C. Baktash, P.-F. Hua, B. Cederwall, P. Fallon, C.J. Gross, H.-Q. Jin, M. Korolija, I.Y. Lee, A.O. Macchiavelli, M.R. Maier, W. Rathbun, D.W. Stracener, and T.R. Werner (1995) Evidence for Hyperdeformation in ^{147}Gd. *Phys. Rev. Lett.* **74** 5186
DOI: https://link.aps.org/doi/10.1103/PhysRevLett.74.5186.

[5] A. Krasznahorkay, M. Hunyadi, M.N. Harakeh, M. Csatlós, T. Faestermann, A. Gollwitzer, G. Graw, J. Gulyás, D. Habs, R. Hertenberger, H.J. Maier, Z. Máté, D. Rudolph, P. Thirolf, J. Timár, and B.D. Valnion (1998) Experimental Evidence for Hyperdeformed States in U Isotopes. *Phys. Rev. Lett.* **80** 2073
DOI: https://link.aps.org/doi/10.1103/PhysRevLett.80.2073.

[6] H. Morinaga (1956) Interpretation of Some of the Excited States of $4n$ Self-Conjugate Nuclei. *Phys. Rev.* **101** 254
DOI: https://link.aps.org/doi/10.1103/PhysRev.101.254.

[7] Y. Fujiwara, H. Horiuchi, K. Ikeda, M. Kamimura, K. Kato, Y. Suzuki, and E. Uegaki (1980) Chapter II. Comprehensive Study of Alpha-Nuclei. *Prog. Theor. Phys.* **68** 29
DOI: http://dx.doi.org/10.1143/PTPS.68.29.

[8] A. Tohsaki, H. Horiuchi, P. Schuck, and G. Röpke (2001) Alpha Cluster Condensation in ^{12}C and ^{16}O. *Phys. Rev. Lett.* **87** 192501
DOI: https://link.aps.org/doi/10.1103/PhysRevLett.87.192501.

[9] T. Suhara, Y. Funaki, B. Zhou, H. Horiuchi, and A. Tohsaki (2014) One-Dimensional α Condensation of α-Linear-Chain States in ^{12}C and ^{16}O. *Phys. Rev. Lett.* **112** 062501
DOI: https://link.aps.org/doi/10.1103/PhysRevLett.112.062501.

[10] P.W. Zhao, N. Itagaki, and J. Meng (2015) Rod-shaped Nuclei at Extreme Spin and Isospin. *Phys. Rev. Lett.* **115** 022501
DOI: http://link.aps.org/doi/10.1103/PhysRevLett.115.022501.

[11] Z.X. Ren, S.Q. Zhang, P.W. Zhao, N. Itagaki, J.A. Maruhn, and J. Meng (2019) Stability of the linear chain structure for ^{12}C in covariant density functional theory on a 3D lattice. *Sci. China-Phys. Mech. Astron.* **62** 112062
DOI: https://doi.org/10.1007/s11433-019-9412-3.

[12] L. Liu and P.-W. Zhao (2012) α-cluster structure of 12 C and 16 O in the covariant density functional theory with a shell-model-like approach. *Chin. Phys. C* **36** 818
DOI: https://doi.org/10.1088%2F1674-1137%2F36%2F9%2F004.

[13] H. Horiuchi (1975) Many-Cluster Problem by the Orthogonality Condition Model: General Discussion and 12C Problem. *Prog. Theor. Phys.* **53** 447
DOI: https://doi.org/10.1143/PTP.53.447.

[14] A.V. Afanasjev and H. Abusara (2018) From cluster structures to nuclear molecules: The role of nodal structure of the single-particle wave functions. *Phys. Rev. C* **97** 024329
DOI: https://link.aps.org/doi/10.1103/PhysRevC.97.024329.

[15] J.M. Yao, N. Itagaki, and J. Meng (2014) Searching for a 4α linear-chain structure in excited states of ^{16}O with covariant density functional theory. *Phys. Rev. C* **90** 054307
DOI: http://link.aps.org/doi/10.1103/PhysRevC.90.054307.

[16] P. Chevallier, F. Scheibling, G. Goldring, I. Plesser, and M.W. Sachs (1967) Breakup of O^{16} into Be^8+Be^8. *Phys. Rev.* **160** 827
DOI: https://link.aps.org/doi/10.1103/PhysRev.160.827.

[17] T. Ichikawa, J.A. Maruhn, N. Itagaki, and S. Ohkubo (2011) Linear Chain Structure of Four-α Clusters in ^{16}O. *Phys. Rev. Lett.* **107** 112501
DOI: https://link.aps.org/doi/10.1103/PhysRevLett.107.112501.

[18] A.H. Wuosmaa, R.R. Betts, B.B. Back, M. Freer, B.G. Glagola, Th. Happ, D.J. Henderson, P. Wilt, and I.G. Bearden (1992) Evidence for alpha-particle chain configurations in ^{24}Mg. *Phys. Rev. Lett.* **68** 1295
DOI: https://link.aps.org/doi/10.1103/PhysRevLett.68.1295.

[19] W.D. M. Rae, A.C. Merchant, and B. Buck (1992) The shape eigenstate: A new kind of resonance. *Phys. Rev. Lett.* **69** 3709
DOI: https://link.aps.org/doi/10.1103/PhysRevLett.69.3709.

[20] Y. Iwata, T. Ichikawa, N. Itagaki, J.A. Maruhn, and T. Otsuka (2015) Examination of the stability of a rod-shaped structure in ^{24}Mg. *Phys. Rev. C* **92** 011303(R)
DOI: https://link.aps.org/doi/10.1103/PhysRevC.92.011303.

[21] T. Inakura and S. Mizutori (2018) Rod-shaped rotational states in $N = Z$ even-even nuclei from ^{12}C to ^{32}S. *Phys. Rev. C* **98** 044312
DOI: https://link.aps.org/doi/10.1103/PhysRevC.98.044312.

[22] N. Itagaki, S. Okabe, K. Ikeda, and I. Tanihata (2001) Molecular-orbital structure in neutron-rich C isotopes. *Phys. Rev. C* **64** 014301
DOI: https://link.aps.org/doi/10.1103/PhysRevC.64.014301.

[23] D.H. Wilkinson (1986) Alpha-neutron rings and chains. *Nucl. Phys. A* **452** 296
DOI: http://www.sciencedirect.com/science/article/pii/0375947486903118.

[24] M. Freer, H. Horiuchi, Y. Kanada-En'yo, D. Lee, and U.-G. Meißner (2018) Microscopic clustering in light nuclei. *Rev. Mod. Phys.* **90** 035004
DOI: https://link.aps.org/doi/10.1103/RevModPhys.90.035004.

[25] Z.X. Ren, S.Q. Zhang, and J. Meng (2017) Solving Dirac equations on a 3D lattice with inverse Hamiltonian and spectral methods. *Phys. Rev. C* **95** 024313
DOI: https://link.aps.org/doi/10.1103/PhysRevC.95.024313.

[26] Z.X. Ren, P.W. Zhao, and J. Meng *to be published*.